MICROWAVE-ASSISTED SYNTHESIS OF CARBON-DOPED CHITOSAN HYDROGELS

Anita Wójcik[1,a], Natalia Wacławik[1,b], Marek Piątkowski[1,c,*]

[1] – Department of Biotechnology and Physical Chemistry,
Faculty of Chemical Engineering and Technology, Cracow University of Technology,
Warszawska 24 Str., 31-155 Cracow, Poland
[a] – ORCID: 0009-0001-2356-0874, [b] – ORCID: 0009-0007-6886-3514,
[c] – ORCID: 0000-0001-9637-1284
**corresponding author: marek.piatkowski@pk.edu.pl*

Abstract

The research focused on analysis of water sorption capacity of carbon-doped and undoped chitosan hydrogels cured with different acids: oxalic acid, citric acid, ascorbic acid, and aspartic acid, synthesised under microwave irradiation. The hydrogels were doped with carbon prepared from brewer's spent grains. The doping effect on the water sorption properties was determined. The results indicate significant differences in water sorption capacity between the undoped and doped hydrogels. The study is significantly important, as it explores the potential of modifying hydrogels to improve their water absorption capacity, a property that is crucial for various industrial applications. The ability to enhance the sorption characteristics of hydrogels through modification or additives can lead to advancements in fields such as agriculture, biomedical engineering, and environmental protection.

Keywords: *chitosan hydrogels, microwave-assisted synthesis, modification, spent grains*

Received: 31.03.2025
Accepted: 31.07.2025

1. Introduction

Chitin and chitosan (CS) are biopolymers obtained from crustacean shells and are structurally similar to cellulose [1]. Chitosan is a linear biopolymer composed of randomly distributed 2-amino-2-deoxy-β-D-glucopyranose (D-glucosamine) and *N*-acetyl-2-amino-2-deoxy-β-D-glucopyranose (*N*-acetyl-D-glucosamine) with β-(1→4) glycosidic linkages. The content of these two units in the chitosan chain defines the degree of deacetylation [2]. Chitosan is obtained from chitin by a deacetylation reaction carried out chemically (with the use of sodium hydroxide) or enzymatically (with the use of chitin deacetylase) [3]. Chitosan does not demonstrate toxic effects in the environment, which allows its safe use in the purification of water reservoirs from heavy metals [4]. Chitosan hydrogels, because of their ability to hold large amounts of water, can also be used as components of horticultural substrates [5]. This feature has a beneficial effect on plants when the soil is highly hydrated. Water in such hydrogels is not strongly bound to the material network; thus, it can be taken up by the plant roots when there is a water shortage in the soil. Additionally, the use of hydrogels also allows the retention and return of nutrients [6].

A variety of polymers can be used to deliver drugs to the human body [7]. The most promising group in terms of biocompatibility and biodegradability are biopolymers and biomaterials, such as chitosan and its derivatives [8]. The use of chitosan in medicine and pharmacy shortens the wound healing process due to its positive effect on the processes of new blood vessel formation from pre-existing blood vessels and scar tissue formation [9]. Chitosan affects the activation of macrophages and the stimulation of cell growth and proliferation, which makes it unique from other polymers used in the production of dressing materials [10].

Hydrogel membranes are used in the manufacture of dressing materials. They increase mechanical strength and have the ability to inhibit the proliferation of bacteria in close contact with the damaged skin layer. Chitosan/sodium alginate polyelectrolyte complexes are used to obtain membranes by solvent casting and evaporation. This method allows three types of water to be defined by DSC studies: free water that is freeze-thawed, polymer-bound water that is freeze-thawed and polymer-bound water that is not freeze-thawed [11].

The method of obtaining hydrogels and the conditions under which the process is carried out have a major influence on the final structure of the resulting hydrogel [12]. The structure of the hydrogel allows the molecules of the substance to diffuse into and out of the hydrogel. This feature opens up the possibility of using them as drug carriers. Therapeutic compounds can thus be delivered to selected locations in the body or targeted to specific tissues [13]. The combination of chitosan, a biocompatible polysaccharide, with carboxylic acids as crosslinkers under microwave radiation has garnered increasing interest in designing smart hydrogels for biomedical and environmental applications. Chitosan-based aerogels intercalated with clay (rectorite) and carbonised under thermal conditions showed strong microwave absorption, indirectly contributing to the materials science side of microwave-hydrogel research [14]. Raspo *et al.* prepared gallic acid-crosslinked chitosan films thermally treated at specific energies and revealed how thermal control affects crosslinking density and film homogeneity [15].

The main aim of the study was the determination of the water sorption capacity of undoped and carbon-doped chitosan-based hydrogels in terms of further industrial applications, e.g., as components of horticultural substrates.

2. Materials and Methods

2.1. Materials

In this study, the following materials were used: chitosan, CS (degree of deacetylation 85%, molecular weight 100,000 - 300,000 g/mol, Qingdao Sunrise Biotechnology, China), D,L-aspartic acid, citric acid monohydrate (min. 99.5% purity), L(+)-ascorbic acid (pure grade), oxalic acid dihydrate (min. 99.5% purity), and ethylene glycol (pure grade) (Pol-Aura, Poland). The carbon obtained from the brewer's spent grain from brewery filtration was also used.

2.2. Carbon preparation

The brewer's spent grain was collected from the brewery filtration tank and dried in a laboratory oven at 70°C for 3 hours. A sufficient amount of the dried product was weighed and placed into a crucible to fill two-thirds of its volume. The crucible was then sealed with a lid, placed in a heating mantle, and positioned deep under the fume hood. Pyrolysis was conducted for 60 minutes. After the process was completed, the crucible was allowed to cool for approximately 15 minutes. The obtained carbon was transferred to a mortar to homogenise.

2.3. Synthesis of Carbon-Undoped Chitosan Hydrogels

In the synthesis of carbon-undoped chitosan-based hydrogels, 0.5 g of chitosan was used for each composition. The organic acids (OA) used in the process included aspartic acid (Asp), citric acid (Cit), ascorbic acid (Asc), and oxalic acid (Oxl). The 1:1 and 1:2 molar ratios of polymer to selected acid were applied, calculated according to 1 mer of chitosan. Ethylene glycol (EG) was used as a high-boiling solvent. During the synthesis, the following synthesis parameters were varied: the volume of water serving as the reaction medium (25 mL or 15 mL), the volume of ethylene glycol used as a solvent (10 mL or 5 mL), and the reaction time, which was adjusted based on the behaviour of the mixture during microwave exposure.

Specifically, a precise amount of the selected OA was weighed and dissolved in the predetermined volume of water while heating the mixture under a cover. Subsequently, 0.5 g of CS was added to the solution, and the mixture was maintained at an elevated temperature until a homogeneous solution was obtained. Once homogenisation was achieved, the appropriate amount of ethylene glycol was added, and the mixture was thoroughly stirred. Depending on the OA used, the initial pH of the reaction mixture equals 4.5 - 5.5. The synthesis process was conducted in a Qilive Q.6865/152345/ D90N30ESLRIII-ZWA microwave reactor (power 1400 W) until hydrogel formation was observed, indicated by the appearance of a light brown colouration and a characteristic caramel-like odour (Table 1). The obtained hydrogel was cooled, immersed in 100 mL of distilled water and left for 20 minutes. Afterwards, the hydrogel was filtered and subjected to five successive washings with distilled water (100 mL per wash) until neutral pH (the pH after synthesis was ca. 6.5). Then, the samples were frozen and lyophilised for 3 days at a temperature of –80ºC.

The resulting materials were weighed to identify samples with the highest mass. The analysis of optimal synthesis conditions resulting in optimal porosity, structural integrity, and a dry, sponge-like consistency was performed. Based on final dry mass, structural stability, and minimal water and ethylene glycol content, samples with the most favourable physicochemical properties were selected for further investigations. The target hydrogel was expected to exhibit high yield, mechanical durability, and a porous, sponge-like surface. In subsequent research stages, a comparative analysis of hydrogels synthesised

with the four different acids was planned. To this end, one representative hydrogel sample was selected from each acid synthesis: aspartic acid, ascorbic acid, oxalic acid, and citric acid. The composition of the selected hydrogels is provided in Table 1, while their images are given in Figure 1.

Table 1. Synthesis parameters of carbon-undoped hydrogels selected for further studies.

Hydrogel name	Acid (OA)	CS:OA molar ratio	EG volume [mL]	H_2O volume [mL]	t [s]
Asp	aspartic acid	1:2	10	25	300
Cit	citric acid	1:1	5	15	180
Asc	ascorbic acid	1:2	5	15	180
Oxl	oxalic acid	1:2	10	15	210

Note. t, synthesis time.

Figure 1. Samples of carbon-undoped chitosan hydrogels.

2.4. Synthesis of Carbon-Doped Chitosan Hydrogels

The synthesis of carbon-doped chitosan-based hydrogels was based on the same procedure described in section 2.3. The molar ratios and preparation conditions remained identical to those in the earlier formulations. The key modification in this case was the addition of carbon prepared from a brewer's spent grain to the hydrogel composition before synthesis in the microwave reactor (Table 2). It should be noted that different synthesis times were needed for the carbon-doped samples to obtain the hydrogel. Figure 2 presents the images of the synthesised carbon-doped hydrogels.

Table 2. Synthesis parameters of carbon-doped hydrogels.

Hydrogel name	Carbon mass [g]	CS:OA molar ratio	EG volume [mL]	H_2O volume [mL]	t [s]
Asp'	0.5055	1:2	10	25	240
Cit'	0.5037	1:1	5	15	140
Asc'	0.5154	1:2	5	15	150
Oxl'	0.5109	1:2	10	15	210

Note. t, synthesis time.

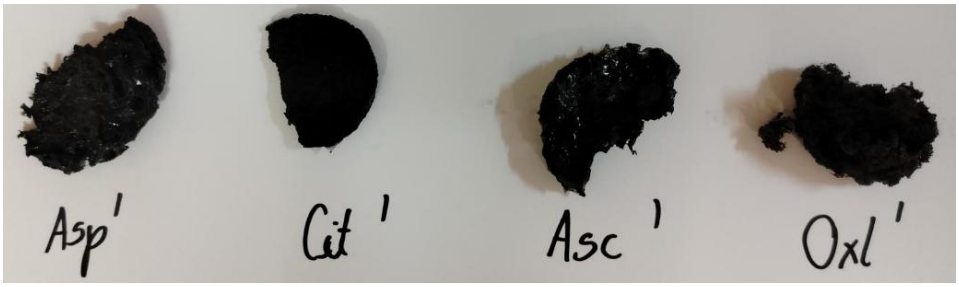

Figure 2. Samples of carbon-doped chitosan hydrogels.

2.5. Determination of the Hydrogels' Water Sorption Capacity

An analysis of the water sorption properties of chitosan-based hydrogels, both doped and undoped, was performed by immersing the hydrogels in distilled water and weighing the material for 6 h at 1 h intervals. It was noted after 6 h that the hydrogels' weight started to decrease, which indicates their degradation; thus, no further measurements were taken. Before weighing, the wet container with the sample was taken out from the solution and put on a paper towel to absorb excess water. The maximum sorption capacity (SC_{max}) was calculated based on the formula:

$$SC_{max} = \frac{m_s - m_d}{m_d} \cdot 100\% \quad (1)$$

where:
m_s – the mass of the swollen hydrogel [g];
m_d – the mass of the dry hydrogel [g].

All the measurements were carried out in triplicate. The data were presented as mean values with a standard deviation, which was given in the figures as error bars.

2.6. Analysis of the Hydrogels' Structure Using ATR-FTIR Spectroscopy

An Attenuated Total Reflectance-Fourier transform infrared spectroscopy (ATR-FTIR) analysis was performed to examine the structure of chitosan-based hydrogels. Before the analysis, the samples were dried for 2 hours at 120°C. Then, a small amount of the powdered sample was placed on an ATR crystal. Spectra were collected on the IRSpirit spectrophotometer (Shimadzu, Japan) in ATR mode in the 400 - 4000 cm^{-1} range at 8 cm^{-1} resolution, collecting 32 scans. The recorded spectra were analysed to identify characteristic functional groups, assess possible chemical modifications, and evaluate intermolecular interactions within the hydrogel matrix.

The analysis also involved a comparison between undoped and carbon-doped chitosan-based hydrogels. This comparison allowed the identification of shifts in absorption bands, changes in functional groups, and potential alterations in the molecular structure due to the modification process. The differences observed in the IR spectra provided insight into the chemical composition and structural characteristics of the undoped and carbon-doped hydrogels.

3. Results and Discussion

Differences in the properties of the synthesised carbon-undoped chitosan-based hydrogels were observed depending on the applied acid (Figure 1). Hydrogels synthesised with aspartic acid exhibited a dark caramel colour and a moderately porous, spongy, and elastic structure. Hydrogels synthesised with citric acid had a white colour with creamy or caramel-like streaks in areas of higher microwave intensity, and a moderately porous, spongy, and elastic structure. Hydrogels synthesised with ascorbic acid were characterised by a dark caramel colour, a highly porous, spongy, and elastic structure, and tended to adhere to the container. Finally, hydrogels synthesised with oxalic acid displayed a very dark caramel colour and a highly porous, rigid, and brittle structure.

3.1. Water Sorption Capacity

The results of the water sorption measurements and values of maximum sorption capacities are provided in Figures 3 - 5.

The analysis of undoped hydrogel samples (Figures 3 and 5) reveals significant differences in their maximum sorption capacities, which vary with the OA used. The oxalic acid-based hydrogel exhibited the highest 1857% maximum sorption capacity among the tested undoped hydrogels. The citric acid-based hydrogel also demonstrated a relatively high sorption capacity of 1380%, indicating moderate water retention properties. In contrast, the ascorbic acid-based hydrogel showed a significantly lower sorption capacity of 795%, which may be attributed to structural factors limiting water uptake. The aspartic acid-based hydrogel displayed the lowest sorption capacity, with a value of 504%, suggesting that it is poorly suited for water absorption in its undoped state.

The comparison of the results obtained with carbon-doped hydrogel samples (Figures 4 and 5) indicates considerable differences in their sorption abilities, depending on the OA used. Similar to the results obtained for the undoped hydrogels, the oxalic acid-based carbon-doped one exhibited the highest sorption capacity, reaching 2240%, indicating superior water absorption properties. In turn, the ascorbic acid-based hydrogel demonstrated a high 2141% sorption capacity, only slightly lower than that of the oxalic acid-based hydrogel. The aspartic acid-based hydrogel doped with carbon, with a sorption capacity of 1848%, showed a moderately lower ability to absorb water than Oxl' hydrogels, yet still maintained a strong sorption performance. It should be pointed out that in the case of carbon-doped Oxl', Asc', and Asp' samples, their swelling capacity is higher than the corresponding undoped Oxl, Asc, and Asp samples. This indicates that modification with carbon prepared from brewer's spent grain significantly enhanced the sorption properties of this type of hydrogel. On the contrary, among all tested carbon-doped samples, the citric acid-based hydrogel (Cit') exhibited the lowest sorption capacity of 764%, lower than the Cit sample, suggesting that citric acid modification in combination with carbon prepared from brewer's spent grain negatively impacted water uptake.

Summarising, in most cases, modification with carbon prepared from brewer's spent grain improved the sorption capacity significantly. Among carbon-doped hydrogels of improved water sorption capacities, the best-performing modified sample was an oxalic acid-based hydrogel with SC_{max} = 2240%, while the least effective was an aspartic acid-based hydrogel with SC_{max} = 504%.

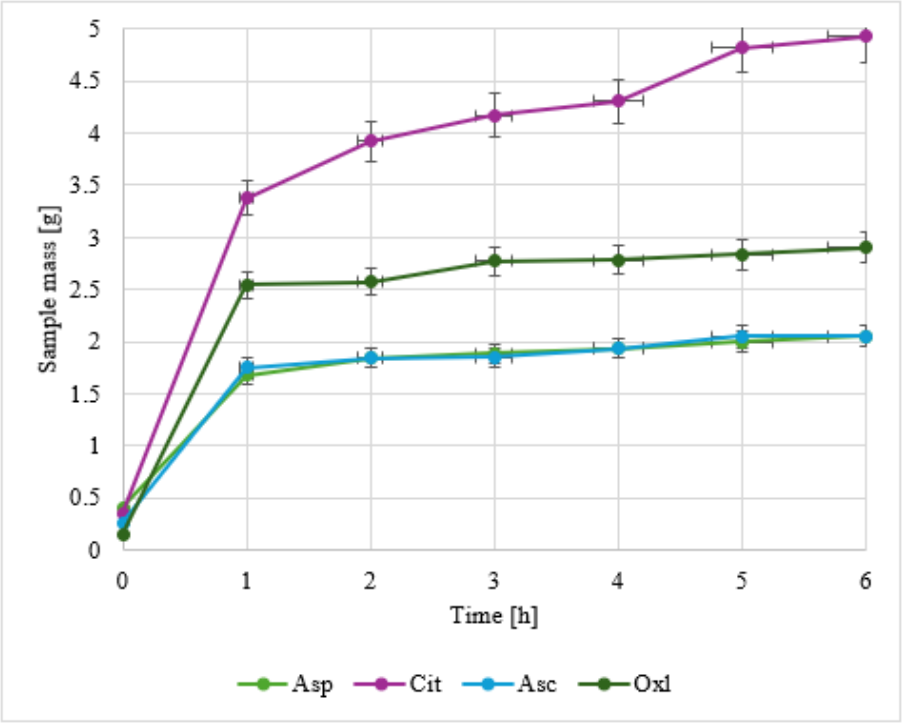

Figure 3. Analysis of the sorption properties of undoped hydrogels.

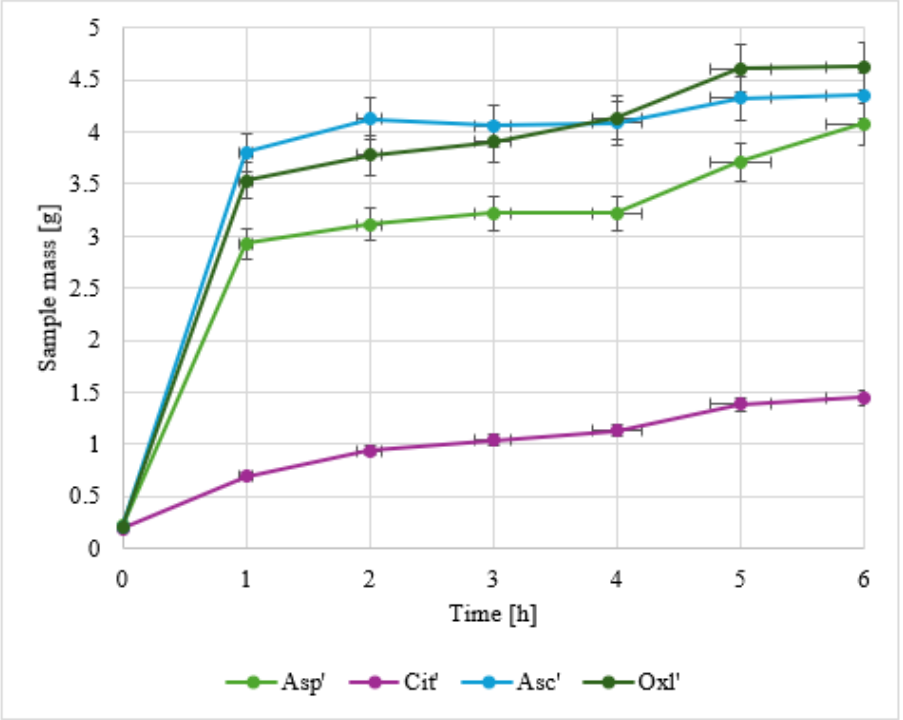

Figure 4. Analysis of the sorption properties of carbon-doped hydrogels.

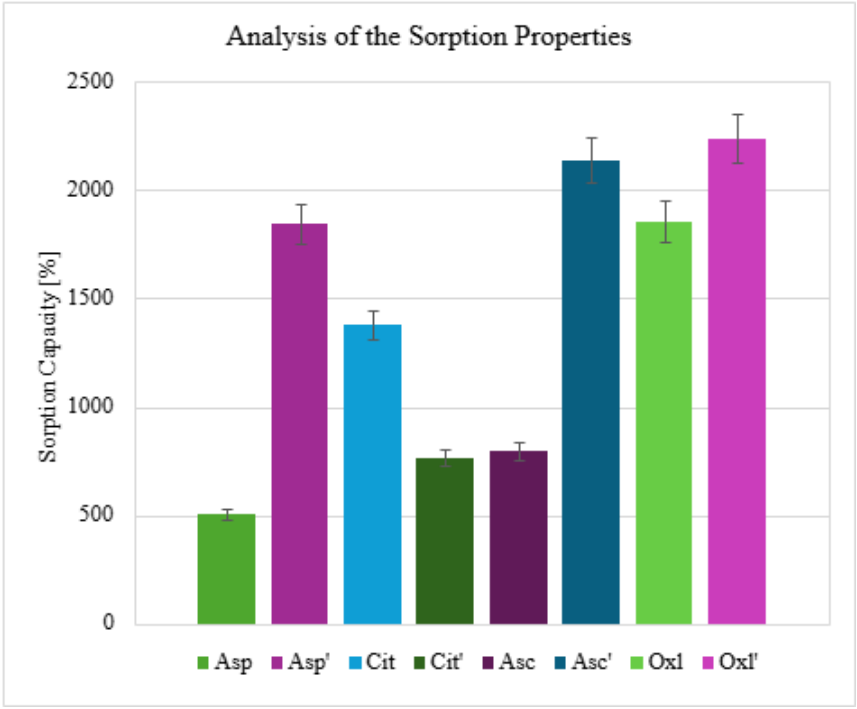

Figure 5. Determination of maximum water sorption capacity of synthesised hydrogels.

3.2. Structure Analysis

In Figure 6, the FTIR spectrum of chitosan is demonstrated. Typical bands with a maximum at 3349 cm^{-1} corresponding to stretching vibrations of OH and NH_2 groups, at 2869, 1419 and 1315 cm^{-1} from symmetric and asymmetric stretching vibrations of methylene and methine groups in chitosan pyranose rings, at 1643 cm^{-1} stretching vibrations in C=O and bending vibrations in N–H of amide groups, at 1374 cm^{-1} from C–H bending vibrations in *N*-acetyl groups, at 1591 and 1151 cm^{-1} characteristic to free amino groups, at 1063 and 1021 cm^{-1} corresponding to glycosidic bonds between chitosan mers, and at 892 cm^{-1} band characteristic to glucopyranose rings can be observed [16].

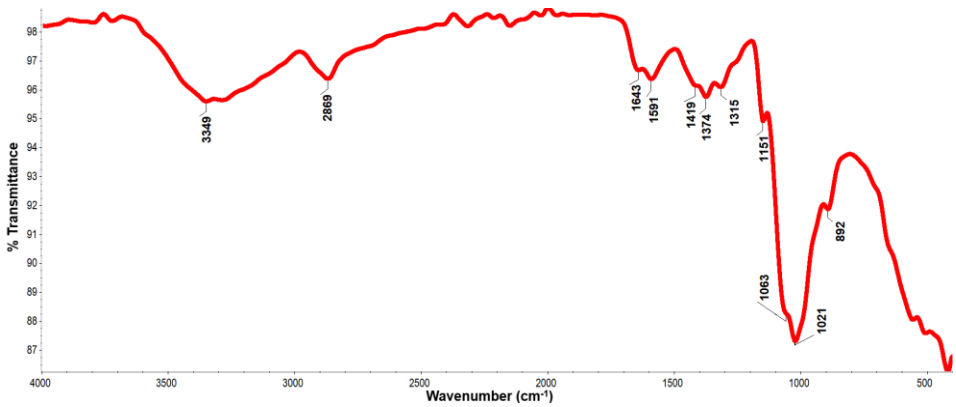

Figure 6. FTIR spectrum of chitosan.

Figure 7 demonstrates the FTIR spectrum of ascorbic acid-based chitosan hydrogel (Asc). Bands characteristic of chitosan with maximum at 2876, 1141, 1077, and 1028 cm^{-1} can be observed. The change in the band's shape and intensity at 3269 cm^{-1} and a new band at 2928 cm^{-1} indicate the incorporation of ethylene glycol into the hydrogel's structure. Moreover, bands characteristic of ascorbic acid with a maximum at 1751 cm^{-1} (carbonyl group), 876 and 759 cm^{-1} (hydroxyl functional in the carboxyl group) can be observed. The intensity of bands with maximum at 1674, 1579, and 1322 cm^{-1} has increased, which proves the formation of amide/ester bonds between chitosan, ascorbic acid, and ethylene glycol [17].

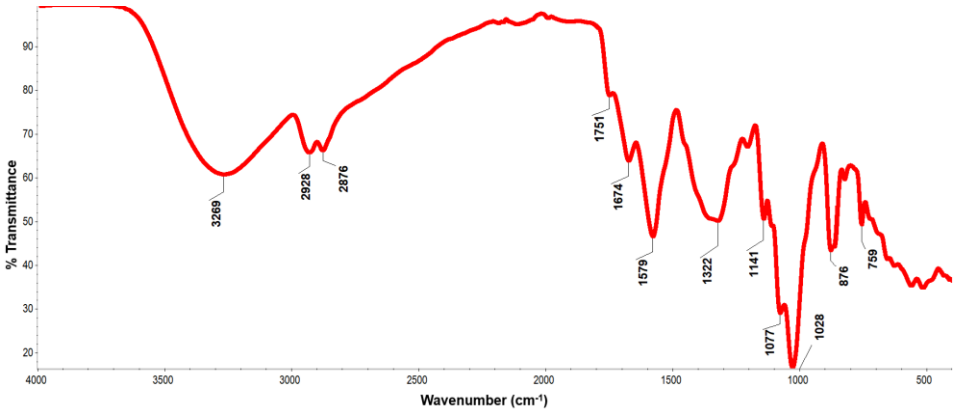

Figure 7. FTIR spectrum of ascorbic acid-based chitosan hydrogel (Asc).

Figure 8 demonstrates the FTIR spectrum of aspartic acid-based chitosan hydrogel (Asp). Bands characteristic of chitosan at 2870, 1154, 1069 and 1028 cm^{-1} can be observed. Similar to Asc (Figure 7), the change in the band's shape and intensity with a maximum at 3228 cm^{-1} and a new band at 2926 cm^{-1} indicate the incorporation of ethylene glycol into the hydrogel's structure. Moreover, bands characteristic of aspartic acid with a maximum at 1707 cm^{-1} (carbonyl group) and 880 cm^{-1} (hydroxyl functional in the carboxyl group) can be observed. The increase in intensity of bands with a maximum at 1571 and 1381 cm^{-1} proves the formation of amide/ester bonds between chitosan, aspartic acid and ethylene glycol.

Figure 9 demonstrates the FTIR spectrum of citric acid-based chitosan hydrogel (Cit). Bands characteristic of chitosan at 2874, 1152, 1077, and 1032 cm^{-1} can be observed. The change in the shape and the intensity of the band with a maximum at 3285 cm^{-1} and a new band at 2932 cm^{-1} indicate the incorporation of ethylene glycol. Moreover, bands characteristic of citric acid with a maximum at 1711 cm^{-1} (carbonyl group) and 880 cm^{-1} (hydroxyl functional in the carboxyl group) can be observed. The intensity of bands with maxima at 1579 and 1381 cm^{-1} has increased. This change indicates the formation of amide bonds between chitosan, aspartic acid and ethylene glycol. Moreover, a characteristic band at 1202 cm^{-1}, resulting from the presence of ester bonds, can be noted.

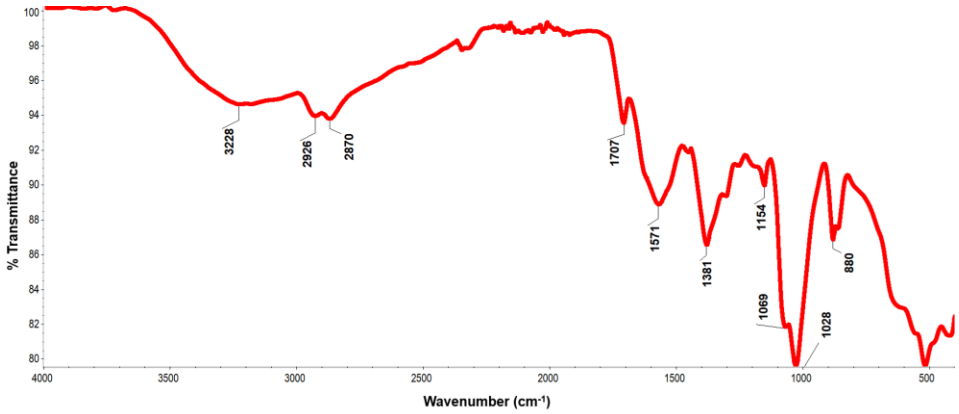

Figure 8. FTIR spectrum of aspartic acid-based chitosan hydrogel (Asp).

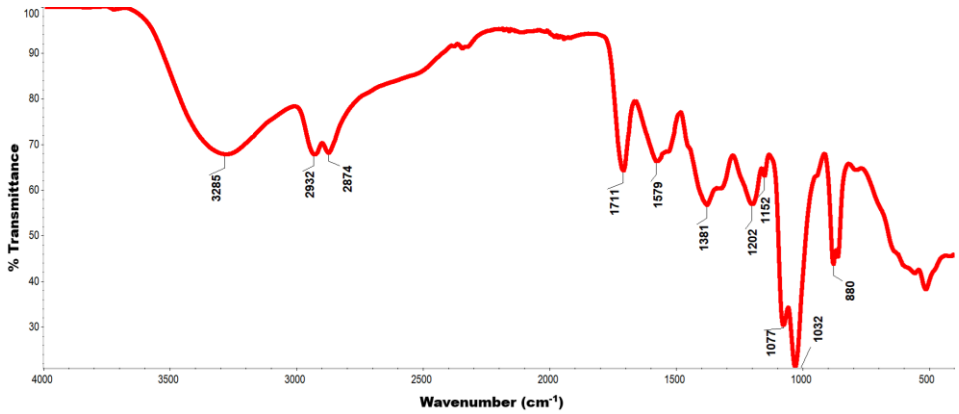

Figure 9. FTIR spectrum of citric acid-based chitosan hydrogel (Cit).

Figure 10 demonstrates the FTIR spectrum of oxalic acid-based chitosan hydrogel. Bands characteristic of chitosan at 2874, 1154, 1064 and 1024 cm^{-1} can be observed. As previously discussed for Asc, Asp and Cit hydrogels, the change in the band's shape and intensity with a maximum at 3259 cm^{-1} and a new band at 2932 cm^{-1} indicate the incorporation of ethylene glycol into the hydrogel's structure. Moreover, bands characteristic of oxalic acid with a maximum at 1737 cm^{-1} (carbonyl group) and at 882 and 763 cm^{-1} (hydroxyl functional in the carboxyl group) can be observed. The increase in 1634, 1534 and 1376 cm^{-1} bands intensity proves the formation of amide bonds between chitosan, oxalic acid and ethylene glycol. Moreover, a band with a maximum at 1302 and 1200 cm^{-1} characteristic of ester bonds can be seen.

In Figure 11, FTIR spectra of chitosan and undoped hydrogels are compared, demonstrating differences in band positions and thus also the differences in chemical composition depending on the OA applied during the synthesis. In all hydrogels, bands characteristic of amide/ester bond formation and those confirming the incorporation of ethylene glycol into the hydrogel structure can be observed. The differences in the 3200 - 3500 cm^{-1} wavenumber range indicate that hydrogen bonding changes occur upon crosslinking. Increase in the intensity of bands within the 1630 - 1700 (Amide I), 1500 - 1550 cm^{-1} (Amide II), 1200 – 1300, and 1700 - 1750 cm^{-1} (ester bonds) ranges confirms amide and ester bonds formation.

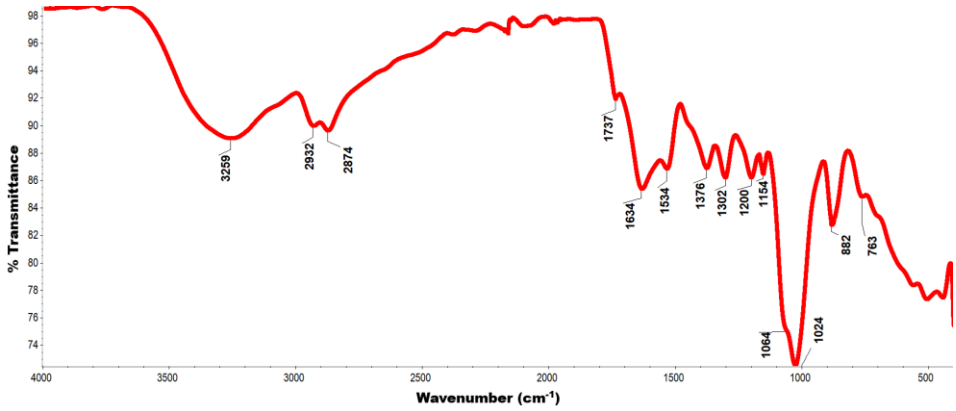

Figure 10. FTIR spectrum of oxalic acid-based chitosan hydrogel (Oxl).

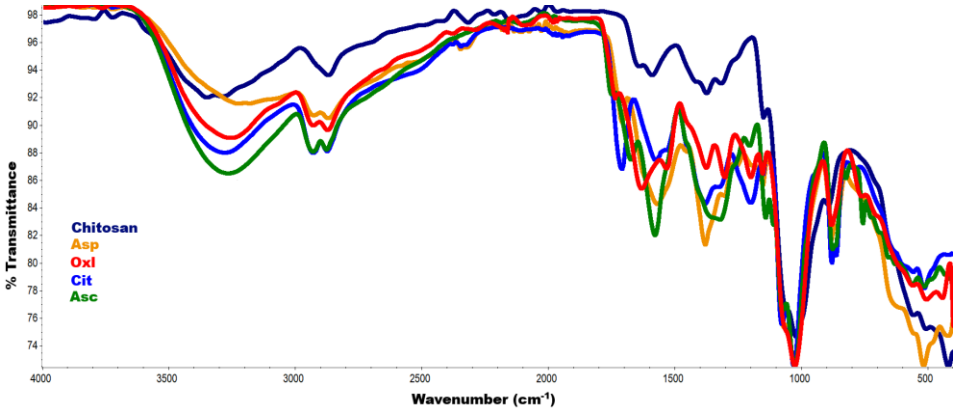

Figure 11. FTIR spectra of pure chitosan and undoped hydrogels.

In Figure 12, FTIR spectra of chitosan and carbon-doped hydrogels are presented, demonstrating differences in vibration bands resulting from variation in chemical composition and structure of hydrogels prepared with different OA. In the spectra of all carbon-doped chitosan hydrogels, bands characteristic of the formed amide/ester bond and the bands confirming incorporation and interactions of ethylene glycol can be observed. In comparison with undoped hydrogels, a shift of the band maximum in the region 3200 - 3500 cm^{-1}, probably due to the formation of additional hydrogen bonds, is observed. Moreover, the intensity of bands around 1580 cm^{-1} (C=C bonds) and 1700 cm^{-1} has increased due to additional carbonyl groups formed during the oxidation of carbon under microwave radiation [18]. In conclusion, it is observed that the incorporation of carbon from brewer's spent grain affects the chemical structure of prepared hydrogels, which can cause differences in water sorption capacity.

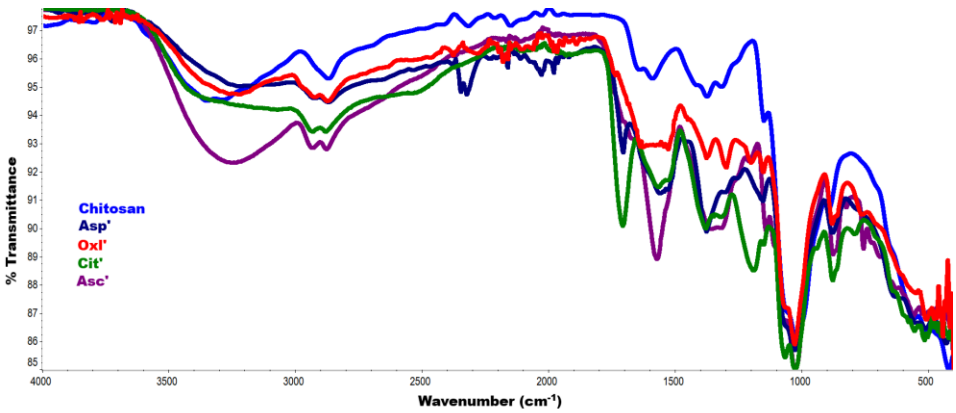

Figure 12. FTIR spectra of pure chitosan and carbon-doped hydrogels.

The FTIR spectra analysis allows us to propose the chemical structure of chitosan hydrogels synthesised through polycondensation reaction with different organic acids and ethylene glycol, as presented in Figure 13.

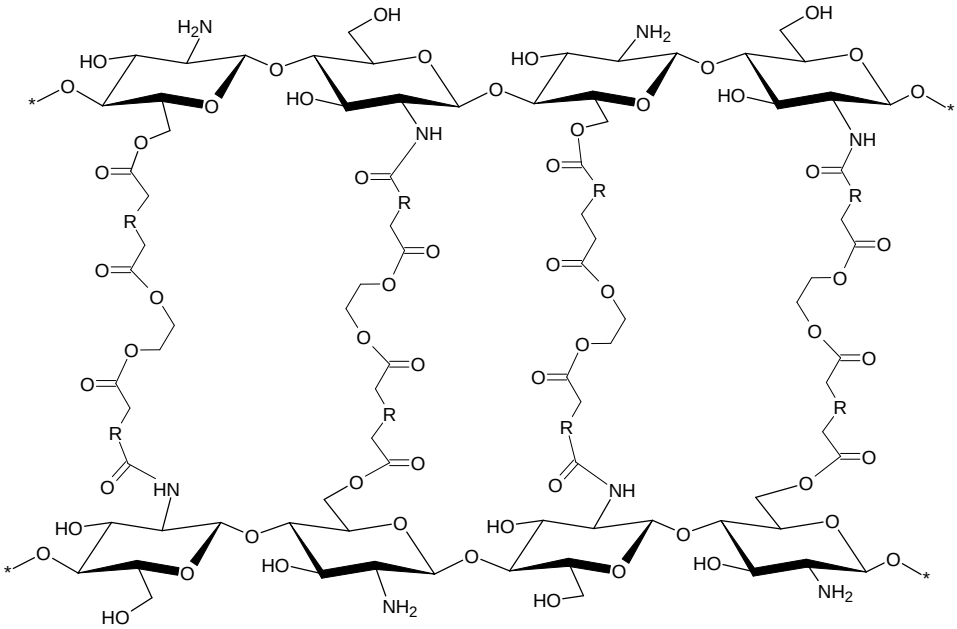

Figure 13. The structure of chitosan hydrogels cured with different organic acids and ethylene glycol (R represents the rest of OA used in the synthesis).

4. Conclusions

The article presents the method of synthesis of chitosan hydrogels crosslinked with different organic acids and ethylene glycol under microwave radiation. The chemical crosslinking of biopolymer chains through the formation of amide and ester bonds was confirmed with FTIR analysis. Moreover, doping the hydrogels with carbon caused a shift

in the position of the vibrational bands, probably due to the formation of additional hydrogen bonding between the hydrogels and carbon, which in turn affected the hydrogels' sorption properties. The comparison between undoped and carbon-doped hydrogel samples clearly highlights the impact of modification on their sorption capacities. In general, the modification with carbon from brewer's spent grain significantly improved the water sorption properties of most synthesised hydrogels. In both its undoped and carbon-doped states, the oxalic acid-based chitosan hydrogel consistently demonstrated the highest sorption capacities, with the carbon-doped sample reaching 2240%. Similarly, the ascorbic acid-based hydrogel exhibited a notable increase in water retention, with its carbon-doped form achieving a sorption capacity of 2141%, compared to 795% in the undoped state. On the other hand, the citric acid-based hydrogel showed a decline in sorption capacity after modification, suggesting that the combination of citric acid and carbon from brewer's spent grain may have negatively affected its water sorption abilities. Aspartic acid-based hydrogel also significantly enhanced its sorption capacity after carbon doping, increasing from 504% to 1848%. Overall, doping hydrogels with carbon from brewer's spent grain is a possible way of improving the water sorption properties of the chitosan/ethylene glycol/OA hydrogels formed under microwave radiation.

5. Acknowledgements

The Authors would like to thank PhD Filip Koper and PhD Wiktor Kasprzyk for the possibility of FTIR analysis, as well as DSc PhD Szczepan Bednarz for the possibility of samples lyophilisation. We would also like to thank Mr Piotr Drochliński and all the Browar Górniczo-Hutniczy (BGH) staff in Kraków for their support with the sample of brewer's spent grain. This research was financed by the National Science Centre, Poland (grant number UMO-2017/26/D/ST8/00979), as well as the National Centre for Science and Development, Poland (grant number LIDER/42/0149/L 9/17/NCBR/2018).

6. References

[1] Cheong KL, Wang LY, Wu DT, Hu DJ, Zhao J, Li SP; (2016) Microwave-Assisted Extraction, Chemical Structures, and Chain Conformation of Polysaccharides from a Novel Cordyceps Sinensis Fungus UM01. J Food Sci 81(9), C2167–C2174. **DOI:** 10.1111/1750-3841.13407

[2] Rinaudo M; (2006) Chitin and Chitosan: Properties and Applications. Prog Polym Sci 31(7), 603–632. **DOI:** 10.1016/j.progpolymsci.2006.06.001

[3] Freier T, Koh HS, Kazazian K, Shoichet MS; (2005) Controlling cell adhesion and degradation of chitosan films by N-acetylation. Biomaterials 26(29), 5872–5878. **DOI:** 10.1016/j.biomaterials.2005.02.033

[4] Kanmani P, Aravind J, Kamaraj M, Sureshbabu P, Karthikeyan S; (2017) Environmental applications of chitosan and cellulosic biopolymers: A comprehensive outlook. Bioresour Technol 242, 295–303. **DOI:** 10.1016/j.biortech.2017.03.119

[5] Oladosu Y, Rafii MY, Arolu F, Chukwu SC, Salisu MA, Fagbohun IK, Muftaudeen TK, Swaray S, Haliru BS; (2022) Superabsorbent polymer hydrogels for sustainable agriculture: A review. Horticulturae 8(7), 605. **DOI:** 10.3390/horticulturae8070605

[6] Bhatt P, Joshi S, Urper Bayram GM, Khati P, Simsek H; (2023) Developments and application of chitosan-based adsorbents for wastewater treatments. Environ Res 226, 115530. **DOI:** 10.1016/j.envres.2023.115530

[7] Desai N, Rana D, Salave S, Gupta R, Patel P, Karunakaran B, Sharma A, Giri J, Benival D, Kommineni N; (2023) Chitosan: A potential biopolymer in drug delivery and biomedical applications. Pharmaceutics 15(4), 1313. **DOI:** 10.3390/pharmaceutics15041313

[8] Klongthong W, Muangsin V, Gowanit C, Muangsin N; (2020) Chitosan biomedical applications for the treatment of viral disease: A data mining model using bibliometric predictive intelligence. J Chem 2020, 6612034. **DOI:** 10.1155/2020/6612034

[9] Maita KC, Avila FR, Torres-Guzman RA, Garcia JP, Eldaly AS, Palmieri L, Emam OS, Ho O, Forte AJ; (2022) Local anti-inflammatory effect and immunomodulatory activity of chitosan-based dressing in skin wound healing: A systematic review. J Clin Transl Res 8(6), 488–498. **DOI:** 10.18053/jctres.08.202206.007

[10] Yazdi MK, Vatanpour V, Taghizadeh A, Taghizadeh M, Ganjali MR, Munir MT, Habibzadeh S, Saeb MR, Ghaedi M; (2020) Hydrogel membranes: A review. Mater Sci Eng C 114, 111023. **DOI:** 10.1016/j.msec.2020.111023

[11] Luz GM, Mano JF; (2010) Mineralized structures in nature: Examples and inspirations for the design of new composite materials and biomaterials. Compos Sci Technol 70(13), 1777–1788. **DOI:** 10.1016/j.compscitech.2010.05.013

[12] Kluczka J; (2023) Chitosan: Structural and chemical modification, properties, and application. Int J Mol Sci 25(1), 554. **DOI:** 10.3390/ijms25010554

[13] Friend DR; (2005) New oral delivery systems for treatment of inflammatory bowel disease. Adv Drug Deliv Rev 57(2), 247–265. **DOI:** 10.1016/j.addr.2004.08.011

[14] Zheng M, Liu F, Yang D, Chen C, Dong X, Deng H; (2025) Chitosan-intercalated rectorite/biomass carbon aerogels with enhanced heterogeneous interfaces for broadband microwave absorption. Chem Eng J 519, 165579. **DOI:** 10.1016/j.cej.2025.165579

[15] Raspo MA, Gomez CG, Andreatta AE; (2025) Thermal treatment inducing the building up of tailor-made chitosan films containing gallic acid. J Polym Sci 63(5), 1197–1204. **DOI:** 10.1002/pol.20240764

[16] Radwan-Pragłowska J, Piątkowski M, Janus Ł, Bogdał D, Matysek D; (2017) Biodegradable, pH-responsive chitosan aerogels for biomedical applications. RSC Adv 7(52), 32960–32965. **DOI:** 10.1039/C6RA27474A

[17] Silverstein RM, Webster FX, Kiemle DJ; (2007) Spektroskopowe metody identyfikacji związków organicznych. Wydawnictwo Naukowe PWN, Warszawa.

[18] Elsayed MA, Zalat OA; (2015) Factor affecting microwave assisted preparation of activated carbon from local raw materials. Int Lett Chem Phys Astron 47, 15–23. **DOI:** 10.56431/p-39xo0w